



Article

# Bandwidth-Enhanced Circularly Polarized Crescent-Shaped Slot Antenna via Circular-Patch Loading

Son Trinh-Van <sup>1</sup>, Youngoo Yang <sup>1</sup>, Kang-Yoon Lee <sup>1</sup>, Yong Serk Kim <sup>2</sup> and Keum Cheol Hwang <sup>1,\*</sup>

<sup>1</sup> Department of Electrical and Computer Engineering, Sungkyunkwan University, Suwon 440-746, Korea; jsonbkhn@gmail.com (S.T.-V.); yang09@skku.edu (Y.Y.); klee@skku.edu (K.-Y.L.)

<sup>2</sup> College of Information and Communication Engineering, Sungkyunkwan University, Suwon 440-746, Korea; yskimasi@skku.edu

\* Correspondence: khwang@skku.edu; Tel.: +82-31-290-7978

Received: 18 February 2019; Accepted: 13 March 2019; Published: 16 March 2019



**Abstract:** This paper presents the crescent-shaped slot antenna loading of a circular patch that greatly enhances a 3 dB axial-ratio (AR) bandwidth. A bent feeding line was introduced and attached to a 50- $\Omega$  microstrip feed line to achieve circular polarization operation. By loading the circular patch into a crescent-shaped slot at a proper position, the 3 dB AR bandwidth is considerably broadened. An antenna prototype with overall dimensions of 50.8  $\times$  50.8  $\times$  0.5 mm<sup>3</sup> is experimentally demonstrated. Measurement results of the fabricated antenna showed a wide  $-10$  dB reflection bandwidth of 92.33% (1.79–4.86 GHz) and a broad 3 dB AR bandwidth of 84.40% (1.89–4.65 GHz). The measured peak gain of the antenna was approximately 4.09 dBic at 2.9 GHz. Good agreement was also achieved between measurement and simulation results.

**Keywords:** broad bandwidth; circular polarization; crescent-shaped slot antenna; microstrip feed line; patch loading

## 1. Introduction

With rapid progress in the field of modern wireless communications, there is increasing demand for compact and broadband antennas [1–3]. The printed-slot antenna is a promising candidate due to its obvious advantages, such as wide impedance bandwidth, low cost, low profile, and ease of fabrication. Moreover, wireless-communication systems with circularly polarized (CP) antennas can provide better orientation-angle flexibility without causing severe polarization mismatch between transmitter and receiver [4–7]. Therefore, there have been many efforts to design broadband CP slot antennas [8–16]. For slot antennas, a typical technique for realizing circular polarization is to implement perturbation structures to the signal line and/or slot. For instance, by having an inverted-L-shaped tuning stub attached to the signal line of a coplanar waveguide (CPW), and implanting a pair of grounded strips in the slot, a 3 dB axial-ratio (AR) bandwidth of 30.36% was achieved [8]. In other work [9], two orthogonal metallic strips, one protruding from the ground plane toward the slot center and the other protruding from the signal line, were used to realize a 3 dB AR bandwidth of 36.01%. By embedding a lightning-shaped feed line and a pair of inverted-L-shaped strips, another antenna [10] attained a 3 dB AR bandwidth of 48.82%. A regular hexagonal slot antenna with an L-shaped monopole reportedly reached a 3 dB AR bandwidth of 50% [11]. Broadband CP operation was also obtained using the slots with special shapes, and the resultant 3 dB AR bandwidths reached 58.66% for an S-shaped slot in Reference [12], and 60.87% for an L-shaped slot [13]. In another design [14], a microstrip-fed

annual ring slot antenna with a pair of grounded hat-shaped patches was introduced, demonstrating a 3 dB AR bandwidth of 65.65%. A symmetric aperture consisting of two diamond-shaped slots fed by a CPW feedline was reported [15], leading to a 3 dB AR bandwidth of around 67.60%. In Reference [16], a falcate-shaped radiating patch and a circular slot were embedded to reach a 3 dB AR bandwidth of 58.7%. Recently, a CP slot antenna with a 3 dB AR bandwidth of 73.33% was realized in a design that used a sickle-shaped printed radiator excited by a straightforward tapered microstrip feed line [17].

In this paper, we propose a broadband CP crescent-shaped slot antenna with enhanced 3 dB AR bandwidth, realized by the loading of a circular patch. To achieve a circular polarization operation, a bent feeding line was attached to a 50- $\Omega$  microstrip feed line. A circular patch was then loaded to a proper position inside the crescent-shaped slot to significantly broaden CP bandwidth. Antenna design was analyzed and optimized using the ANSYS High-Frequency Structure Simulator (HFSS), which is an electromagnetic-wave simulator based on the Finite-Element Method (FEM). The antenna was fabricated on a single substrate; therefore, the fabrication process is easy and cost-effective. A broad 3 dB AR bandwidth of up to 84.40% (1.89–4.65 GHz) was experimentally achieved, which is entirely covered by a measured  $-10$  dB reflection bandwidth of 92.33% (1.79–4.86 GHz). The achieved CP operating-frequency band of the proposed antenna covers the operating bandwidths of several systems, such as Bluetooth/WLAN (2.4–2.484 GHz), LTE Band 1 (2100 MHz), LTE Band 7 (2600 MHz), and some sub-6 GHz bands used in 5G mobile communications (e.g., 3.4–3.8 GHz in Europe, 3.3–3.6 GHz in China, and 3.4–3.7 GHz in Korea). The following sections describe the antenna design in detail and discuss the experiment results to confirm the feasibility of the proposed antenna.

## 2. Antenna Design and Parametric Studies

### 2.1. Antenna Design

Figure 1 presents the configuration of the proposed antenna, consisting of a ground plane with a crescent-shaped slot, circular patch loading, a bent feeding line, and a 50- $\Omega$  microstrip feed line. The ground plane and circular patch loading were printed on the upper layer of a substrate with the square dimensions of  $g_w \times g_w$ . The substrate used in this work was Taconic RF-35 with a thickness of 0.5 mm, relative permittivity ( $\epsilon_r$ ) of 3.5, and a loss tangent ( $\tan\delta$ ) of 0.0019. The crescent-shaped slot consists of a circular slot ( $O$ ) jointed with an elliptical patch ( $E_1$ ).  $O$  has an  $R$  radius, and is centered at the center of the substrate.  $E_1$ , with a semimajor axis of  $r_2$  and a semiminor axis of  $r_3$ , is positioned on the periphery of  $O$  at  $\phi = 45^\circ$ . Circular patch loading  $O_1$  has a  $r_1$  radius and its center is located at the  $-s_x, -s_y$  position, related to the center of  $O$ . The 50- $\Omega$  microstrip feed line with a length of  $l_f$  and a width of  $w_f$ , and the bent feeding line were mounted on the bottom layer of the substrate. The bent feeding line was attached to the 50- $\Omega$  microstrip feed line and is composed of three rectangular strips with dimensions of  $w_1 \times l_1, w_2 \times l_2$ , and  $w_3 \times l_3$ . The upper-right corner of the bent feeding line was mitered with a width of  $w_4$ . The geometrical parameters of the proposed antenna were optimized to maximize the overlapping bandwidth, which is determined by the criteria of  $|S_{11}| < -10$  dB and AR < 3 dB. The optimized geometrical parameters of the proposed antenna are tabulated in Table 1.

**Table 1.** Optimized geometrical parameters of proposed antenna.

Parameter	Value (mm)	Parameter	Value (mm)
$R$	21	$g_w$	50.8
$r_1$	10.63	$w_1$	6.12
$r_2$	11.42	$w_2$	21.45
$r_3$	10.37	$w_3$	36.125
$s_x$	4	$l_1$	1.5
$s_y$	4	$l_2$	2.3
$w_f$	1.12	$l_3$	12.72
$l_f$	4.26	$w_4$	8

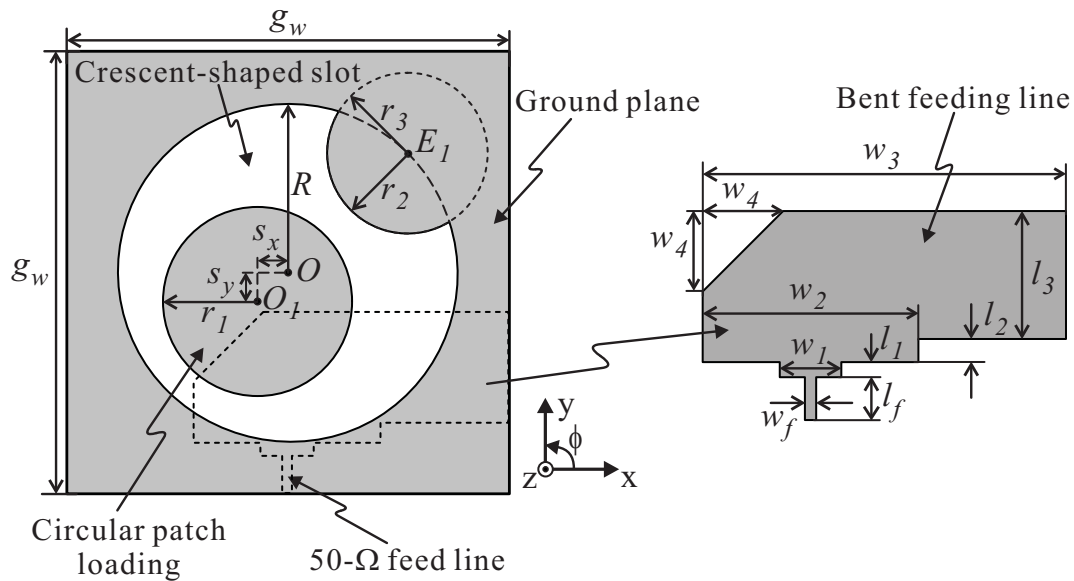


Figure 1. Proposed antenna configuration.

### 2.2. Parametric Studies

Figure 2 presents a comparison of the reflection coefficients and AR performance capabilities of the antenna with circular patch loading (the proposed antenna) and an antenna without circular patch loading (reference antenna). Note that, for a fair comparison, a reference antenna identical in size to the proposed antenna was also optimized to attain good CP behavior. Thus, the geometrical parameters of the reference antenna are slightly different from those of the proposed antenna; they are as follows:  $g_w = 50.8$  mm,  $R = 24$  mm,  $r_2 = 10$  mm,  $r_3 = 10$  mm,  $w_f = 1.12$  mm,  $l_f = 2.36$  mm,  $l_1 = 1$  mm,  $l_2 = 4.3$  mm,  $l_3 = 15.5$  mm,  $w_1 = 6.12$ ,  $w_2 = 21.45$  mm,  $w_3 = 36.125$  mm, and  $w_4 = 8$  mm. As shown in Figure 2, the antenna without circular patch loading had a 3 dB AR bandwidth of 2.83–3.18 GHz (11.65%), which was enclosed within a  $-10$  dB reflection bandwidth of 2.61–4.90 GHz (60.99%). In contrast, by loading with the circular patch inside the crescent-shaped slot, both the reflection and 3 dB AR bandwidths were significantly broadened, resulting in a broad  $-10$  dB reflection bandwidth of 1.80–4.81 GHz (91.07%), and a broad 3 dB bandwidth of 1.80–4.52 GHz (86.08%). An increase of approximately 7.4 times in the 3 dB AR bandwidth was achieved by circular-patch loading.

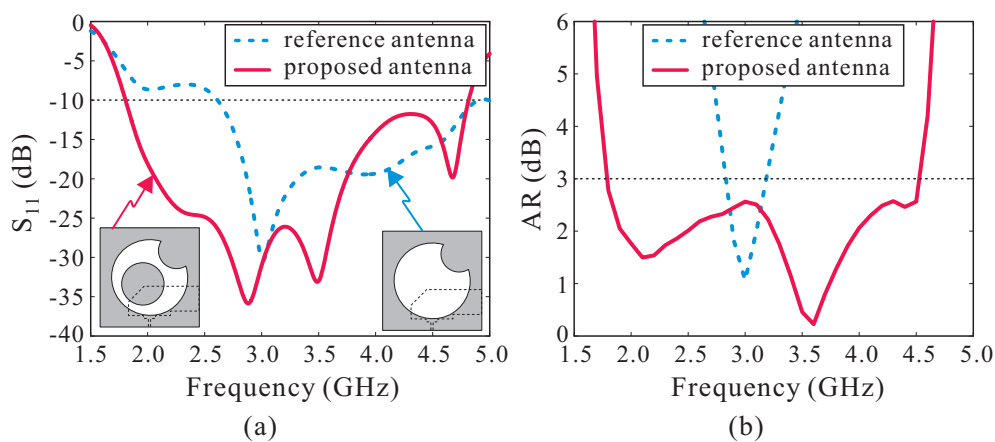
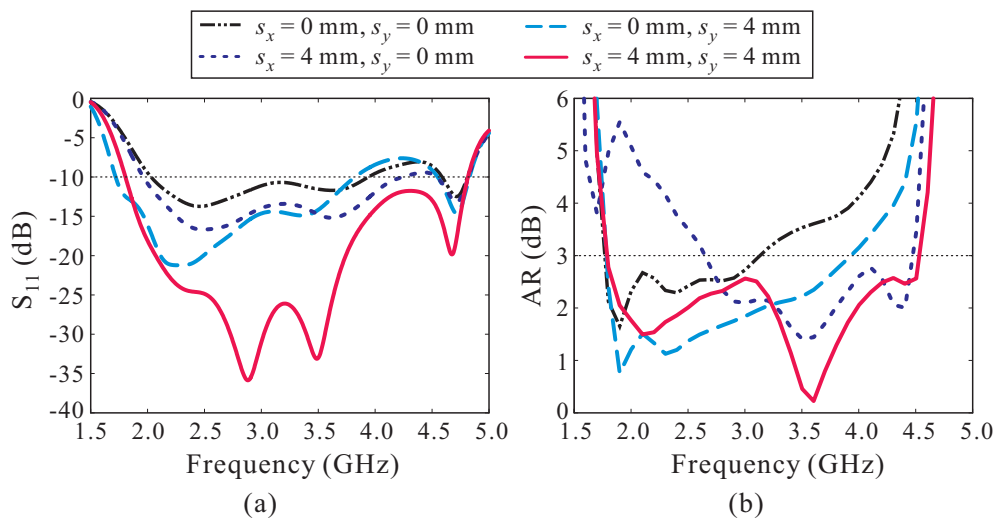


Figure 2. Performance of the antennas with and without circular patch loading: (a) reflection coefficients; (b) Axial Ratios (ARs).

The position of circular-patch loading  $O_1$  in the crescent-shaped slot was also investigated to find its effect on the reflection coefficient and AR performance outcomes. Simulated results are plotted in Figure 3. When the circular patch was located at the center ( $s_x = 0$  mm,  $s_y = 0$  mm), a 3 dB AR bandwidth of 1.92–3.24 GHz (51.16%) was attained. By moving the circular patch along the  $-x$ -axis ( $s_x = 4$  mm,  $s_y = 0$  mm), the 3 dB AR bandwidth was shifted toward the upper frequency range, and the  $-10$  dB reflection bandwidth was improved. When the circular patch was moved along the  $-y$ -axis ( $s_x = 0$  mm,  $s_y = 4$  mm), the  $-10$  dB reflection bandwidth was shifted downward in the lower frequency range, and the 3 dB AR bandwidth was enhanced. The optimal position of the circular patch is offset from the center along both the  $-x$ - and  $-y$ -axes ( $s_x = 4$  mm,  $s_y = 4$  mm), showing the widest 3 dB AR bandwidth entirely enclosed within the  $|S_{11}| < -10$  dB bandwidth.



**Figure 3.** Effect of the position of circular patch loading  $O_1$  on antenna performance: (a) reflection coefficients; (b) ARs.

Figure 4 shows the impact of radius  $r_1$  of circular patch loading  $O_1$  on the reflection coefficients and AR performance capabilities. This figure shows that the  $-10$  dB reflection bandwidth tends to reduce with the decrease in  $r_1$ . In contrast, 3 dB AR bandwidth is enhanced as  $r_1$  decreases. According to this analysis, the best value of  $r_1$  was finally set to 10.63 mm to achieve the widest overlapping bandwidth.

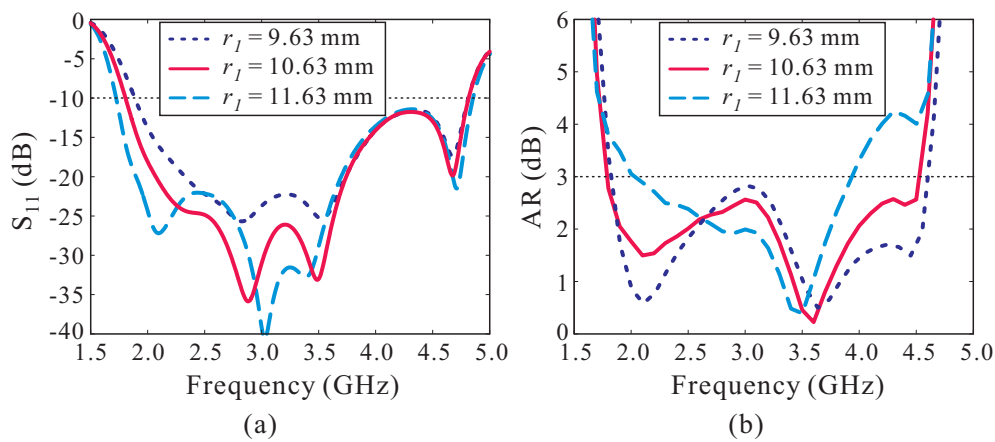


**Figure 4.** Effect of radius  $r_1$  of circular patch loading  $O_1$  on antenna performance: (a) reflection coefficients; (b) ARs.

To visualize how CP radiation is realized, time-varying magnetic-current distribution concentrations in the slot were investigated. Figure 5 displays the magnetic-current distributions at 2.1 and 3.5 GHz, respectively, as observed from the +z-direction. Note that  $M$  indicates the vector sum of all component vectors. As shown in Figure 5a, at  $t = 0$ , vector  $M$  is oriented from the upper-right corner to the lower-left corner. At  $t = T/4$ , vector  $M$  is directed from the lower-right corner to the upper-left corner. This vector is perpendicular to that at  $t = 0$ . In addition, these vectors revolve clockwise as time  $t$  changes. This indicates that the proposed antenna is able to realize left-handed circular polarization (LHCP) in the +z-direction, whereas right-handed circular polarization (RHCP) is generated in the -z-direction. The same outcome was observed at 3.5 GHz, as shown in Figure 5b.

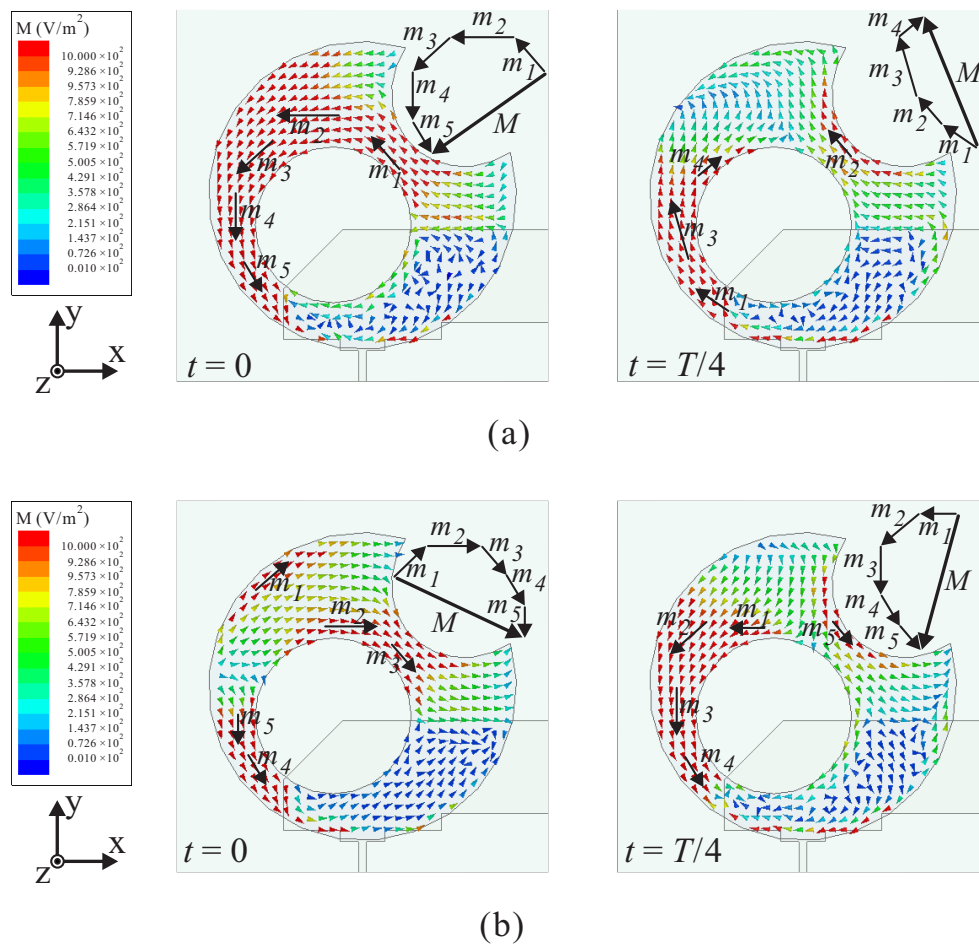


Figure 5. Simulated electric-field distributions in the slot with period  $T$  at: (a) 2.1 GHz; (b) 3.5 GHz.

### 3. Experiment Results

To validate the simulation results, a prototype of the proposed antenna with the optimized parameters, as tabulated in Table 1, was fabricated for measurement. Figure 6 displays the fabricated antenna, which has overall dimensions of  $50.8 \times 50.8 \times 0.5 \text{ mm}^3$ . The reflection coefficient was tested using an Agilent 8510C RF network analyzer. A comparison of the reflection coefficients is illustrated in Figure 7, in which good agreement was apparent between simulation and measurement results. The measured and simulated frequency bandwidths for  $|S_{11}| < -10 \text{ dB}$  were 92.33% (1.79–4.86 GHz) and 91.07% (1.80–4.81 GHz), respectively.

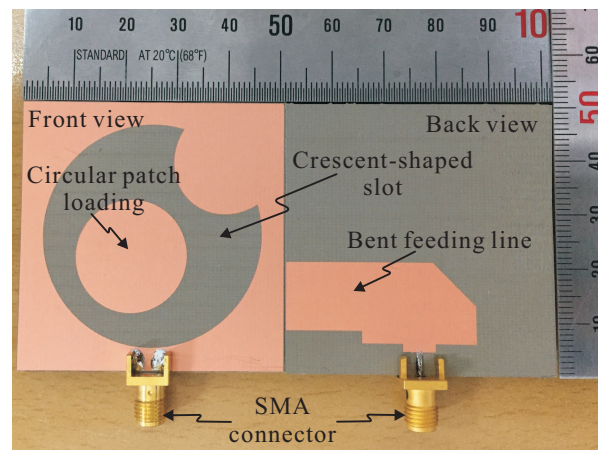


Figure 6. Fabricated antenna.

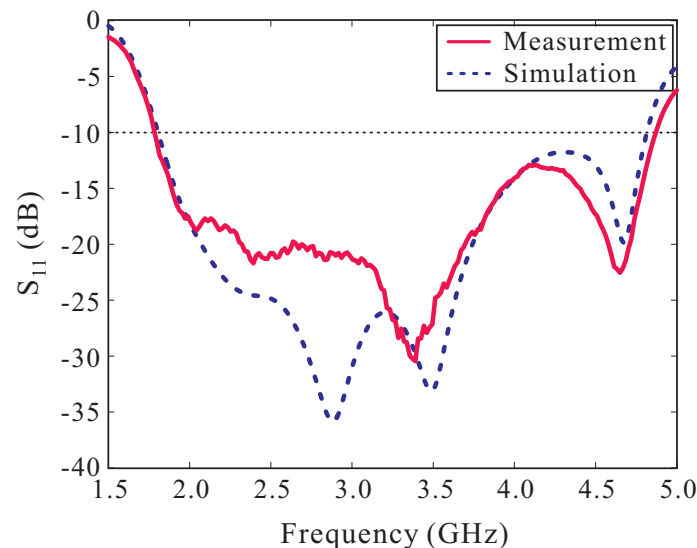
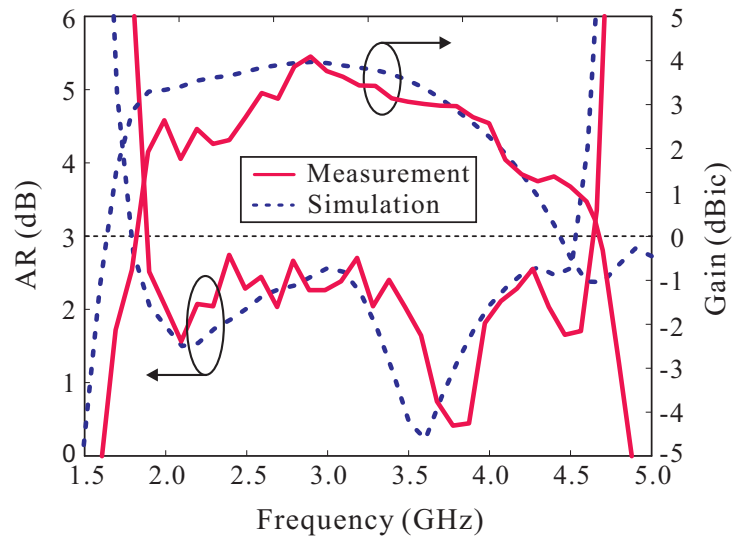
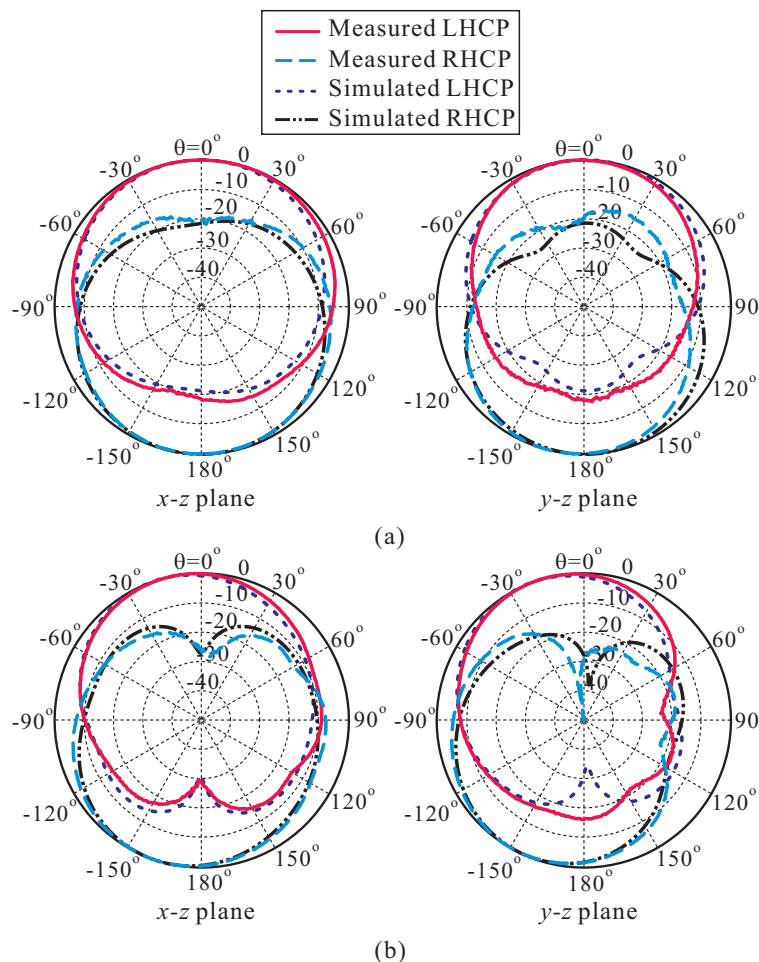


Figure 7. Simulated and measured reflection coefficients of the proposed antenna.

Figure 8 presents the simulated and measured ARs and LHCP gains versus the frequency in  $\theta = 0^\circ$  (broadside direction). The radiation characteristics of the fabricated antenna were measured in an RF anechoic chamber, which was  $5.5 \times 5.5 \times 5.0$  m. A dual-polarized rectangular horn antenna was utilized to acquire the AR and LHCP/RHCP waves. The 3 dB AR bandwidths were 86.08% (1.80–4.52 GHz) and 84.40% (1.89–4.65 GHz) in the simulation and measurement, respectively. It was evident that the 3 dB AR bandwidth was entirely enclosed by the  $-10$  dB reflection bandwidth. In addition, the measured LHCP gains varied from 0.39 to 4.09 dBic within the measured 3 dB AR bandwidth. It was also observed that the antenna gains decreased as frequency increased. This occurred because the main beam was tilted from the broadside direction owing to the asymmetrical configuration of the proposed antenna. The simulated and measured normalized radiation patterns on the two principal planes (the  $x - z$  ( $\phi = 0^\circ$ ) and  $y - z$  ( $\phi = 90^\circ$ ) planes) for 2.1 and 3.7 GHz are displayed in Figure 9. The proposed antenna radiates LHCP in the  $+z$ -direction and RHCP in the  $-z$ -direction. In addition, the radiation patterns at 3.7 GHz are asymmetric and tilted from the broadside direction. Reasonable agreement between simulation and measurement was found. Discrepancy could be attributed to inaccuracies during the fabrication process and experimental tolerances.



**Figure 8.** Simulated and measured ARs, and left-handed circular polarization (LHCP) gains versus frequency.



**Figure 9.** Simulated and measured normalized radiation patterns of the proposed antenna: (a) 2.1 GHz; (b) 3.7 GHz.

Figure 10 plots the simulated and measured ARs versus the observation angle of the proposed antenna at two frequencies, 2.1 and 3.7 GHz. As observed, due to the higher cross-polar levels that

could be found in the radiation patterns at higher frequencies, the 3 dB AR beamwidth became slightly narrower, with an increase in frequency. The measured 3 dB AR beamwidths at 2.1 GHz were 69° and 78° on the  $x - z$  plane and  $y - z$  plane, respectively. At 3.7 GHz, the measured 3 dB AR beamwidths were 55° on the  $x - z$  plane and 76° on the  $y - z$  plane. Furthermore, reasonable agreement was found between simulation and measurement results.

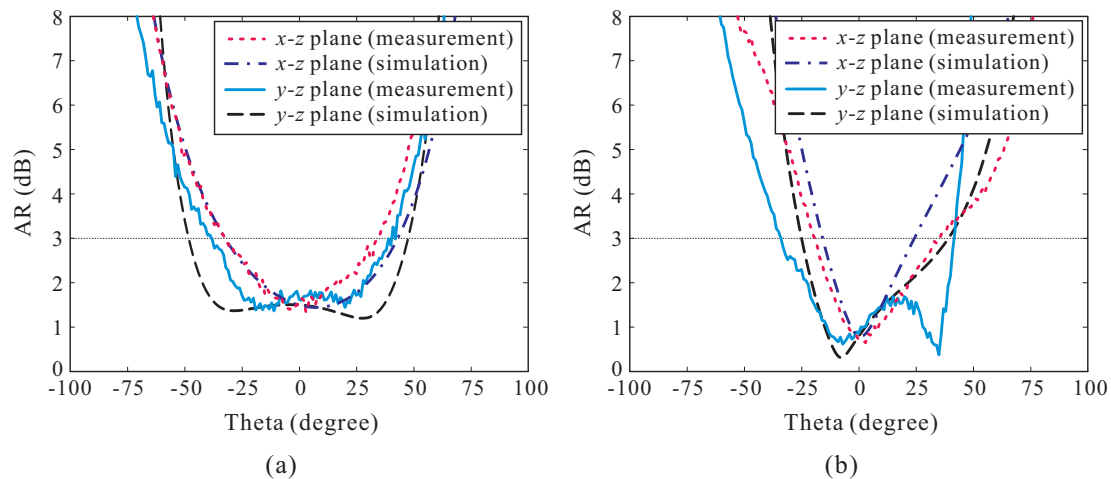


**Figure 10.** Simulated and measured ARs of the proposed antenna versus observation angle: (a) 2.1 GHz; (b) 3.7 GHz.

To evaluate the performance of the antenna, Table 2 summarizes a comparison of the key performance characteristics of this work and the previously published CP slot antennas [8–17]. Note that  $\lambda_c$  represents the wavelength at center frequency  $f_c$  of the 3 dB AR bandwidth. As can be observed in Table 2, the performance of the proposed antenna is competitive, exhibiting broader CP bandwidth as compared to the previous antennas. The proposed antenna also has an acceptable gain for a common slot antenna. Moreover, the antenna size of  $0.55 \times 0.55 \lambda_c^2$  is more compact than in earlier works [9,11–13,15,16].

**Table 2.** Performance comparison with previous broadband circularly polarized (CP) slot antennas.

Ref.	$f_c$ (GHz)	CP Bandwidth * (%)	Antenna Area ( $\lambda_c^2$ )	Peak Gain (dBic)
[8]	2.22	30.63	$0.44 \times 0.44$	4.1
[9]	2.30	36.01	$0.71 \times 0.63$	3.9
[10]	2.75	48.82	$0.55 \times 0.55$	4.2
[11]	3	50	$0.62 \times 0.62$	4.32
[12]	4.03	58.56	$0.73 \times 0.73$	3.55
[13]	4.6	60.87	$0.92 \times 0.92$	2.2
[14]	1.64	65.65	$0.55 \times 0.55$	5.1
[15]	3.625	67.69	$0.72 \times 0.72$	4.0
[16]	4.56	58.7	$0.58 \times 0.58$	6.18
[17]	3.6	73.33	$0.47 \times 0.47$	4.85
This work	3.27	84.40	$0.55 \times 0.55$	4.09

\* The CP bandwidth is determined by the criteria of  $|S_{11}| < -10$  dB and AR < 3 dB.

#### 4. Conclusions

A microstrip-fed broadband CP crescent-shaped slot antenna loaded by a circular patch was presented, fabricated, and tested. The proposed antenna was easily fabricated on a single Taconic RF-35 substrate. The experiment results demonstrated that the proposed antenna has a broad 3 dB AR bandwidth of 84.40% (1.89–4.65 GHz), which is entirely enclosed by a broad  $-10$  dB reflection bandwidth of 92.33% (1.79–4.86 GHz). In addition, the proposed antenna has a compact size of only



$0.55 \times 0.55 \lambda_c^2$ . Therefore, the proposed antenna can feasibly support various wireless-communication systems in which a broadband CP antenna element is necessary.

**Author Contributions:** The presented work was carried out in collaboration of all authors. Son Trinh-Van performed the simulations. Youngoo Yang, Kang-Yoon Lee, Yong Serk Kim, and Keum Cheol Hwang participated to the conception, fabrication and experiment. Son Trinh-Van wrote the paper which was edited by all co-authors.

**Funding:** This research was funded by Institute for Information and Communications Technology Promotion (IITP), grant funded by the Korean Government (MSIP) (10079984, Development of Nonbinding Multimodal Wireless Power-Transfer Technology for Wearable Devices).

**Conflicts of Interest:** The authors declare no conflict of interest.

## References

1. Kubacki, R.; Czyzewski, M.; Laskowski, D. Minkowski island and crossbar fractal microstrip antennas for broadband applications. *Appl. Sci.* **2018**, *8*, 334. [CrossRef]
2. Fukusako, T. Broadband characterization of circularly polarized waveguide antenna using L-shaped probe. *J. Electromagn. Eng. Sci.* **2017**, *17*, 1–8. [CrossRef]
3. Hur, J.; Byun, G.; Choo, H. Design of small CRPA arrays with circular microstrip loops for electromagnetically coupled feed. *J. Electromagn. Eng. Sci.* **2018**, *18*, 129–135. [CrossRef]
4. Trinh-Van, S.; Lee, J.M.; Yang, Y.; Lee, K.-Y.; Hwang, K.C. Improvement of RF wireless power transmission using a circularly polarized retrodirective antenna array with EBG structures. *Appl. Sci.* **2018**, *8*, 324. [CrossRef]
5. Nelaturi, S.; Sarma, N.V.S.N. A compact microstrip patch antenna based on metamaterials for Wi-Fi and WiMAX applications. *J. Electromagn. Eng. Sci.* **2018**, *18*, 182–187. [CrossRef]
6. Kweon, J.-H.; Park, M.-S.; Cho, J.; Jung, K.-Y. FDTD analysis of electromagnetic wave propagation in an inhomogeneous ionosphere under arbitrary-direction geomagnetic field. *J. Electromagn. Eng. Sci.* **2018**, *18*, 212–214. [CrossRef]
7. Guo, L.; Tang, M.-C.; Li, M. A low-profile dual-layer patch antenna with a circular polarizer consisting of dual semicircular resonators. *Sensors* **2018**, *18*, 1773. [CrossRef]
8. Sze, J.-Y.; Wang, J.-C.; Chang, C.C. Axial-ratio bandwidth enhancement of asymmetric-CPW-fed circularly-polarised square slot antenna. *Electron. Lett.* **2008**, *44*, 1048–1049. [CrossRef]
9. Deng, I.-C.; Cheng, J.-B.; Ke, Q.-X.; Chang, J.-R.; Chang, W.-F.; King, Y.-T.A. A circular CPW-fed slot antenna for broadband circularly polarized radiation. *Microw. Opt. Technol. Lett.* **2007**, *49*, 2728–2733. [CrossRef]
10. Sze, J.-Y.; Hsu, C.-I.G.; Chen, Z.-W.; Chang, C.-C. Broadband CPW-fed circularly polarized square slot antenna with lightning-shaped feedline and inverted-L grounded strips. *IEEE Trans. Antennas Propag.* **2010**, *58*, 973–977. [CrossRef]
11. Zhou, S.-W.; Li, P.-H.; Wang, Y.; Feng, W.-H.; Liu, Z.-Q. A CPW-fed broadband circularly polarized regular-hexagonal slot antenna with L-shape monopole. *IEEE Antennas Wirel. Propag. Lett.* **2011**, *10*, 1182–1185. [CrossRef]
12. Li, G.; Zhai, H.; Li, T.; Li, L.; Liang, C. CPW-fed S-shaped slot antenna for broadband circular polarization. *IEEE Antennas Wirel. Propag. Lett.* **2013**, *12*, 619–622. [CrossRef]
13. Li, G.; Zhai, H.; Li, L.; Liang, C. A nesting-L slot with enhanced circularly polarized bandwidth and radiation. *IEEE Antennas Wirel. Propag. Lett.* **2014**, *13*, 225–228.
14. Sze, J.-Y.; Chen, W.-H. Axial-ratio-bandwidth enhancement of a microstrip-line-fed circularly polarized annular-ring slot antenna. *IEEE Trans. Antennas Propag.* **2011**, *59*, 2450–2456. [CrossRef]
15. Nasimuddin; Chen, Z.N.; Qing, X. Symmetric-aperture antenna for broadband circular polarization. *IEEE Trans. Antennas Propag.* **2011**, *59*, 3932–3936. [CrossRef]
16. Le, T.T.; The, V.H.; Park, H.C. Simple and compact slot-patch antenna with broadband circularly polarized radiation. *Microw. Opt. Technol. Lett.* **2016**, *58*, 1634–1641.
17. Samsuzzaman, M.; Islam, M.T. Circularly polarized broadband printed antenna for wireless applications. *Sensors* **2018**, *18*, 4261. [CrossRef]

